

UC Santa Cruz

UC Santa Cruz Previously Published Works

Title

Global Trajectory Tracking for Underactuated VTOL Aerial Vehicles using a Cascade Control Paradigm

Permalink

<https://escholarship.org/uc/item/3094b2jk>

ISBN

9781467357173

Authors

Naldi, Roberto
Furci, Michele
Sanfelice, Ricardo G
et al.

Publication Date

2013-12-01

DOI

10.1109/cdc.2013.6760536

Peer reviewed

Global Trajectory Tracking for Underactuated VTOL Aerial Vehicles using a Cascade Control Paradigm

Roberto Naldi, Michele Furci, Ricardo G. Sanfelice and Lorenzo Marconi

Abstract—This work proposes a feedback control strategy capable of controlling the dynamics of an under-actuated Vertical Take-Off and Landing (VTOL) aerial vehicle to track a desired trajectory globally with respect to the initial conditions. The novelty of the proposed design is the idea of considering a cascade control paradigm in which the attitude dynamics, which are governed by means of a hybrid controller capable of overcoming the well-known topological constraints, and the position dynamics of the vehicle play respectively the role of the inner and of the outer loop. The stability properties of the proposed controller are then derived by analyzing the interconnection between a hybrid system, namely the closed-loop attitude dynamics, and a continuous time system, given by the closed-loop position dynamics. The proposed algorithms are then demonstrated by means of simulations obtained considering a miniature quadrotor prototype.

I. INTRODUCTION

Miniature Vertical Take-Off and Landing (VTOL) aerial systems are currently employed successfully in a large number of applications including surveillance, aerial photography and search and rescue operations [1], among others. One reason for this large success is the high level of maneuverability, which allows to safely perform flight missions even in densely cluttered environments [2] or even to perform advanced robotic tasks [3]. Among the different configurations, this class of systems include helicopters [4], ducted-fan tail-sitters - [5], [6], [7] - and multi-propeller helicopters - [8], [9], [10]. To fully take advantage of the potential of such vehicles, globally stabilizing control designs play a central role.

Several contributions and seminal papers document different approaches to the control design for such a class of under-actuated systems [11], [12], [13]. In [14], almost-global stability results are demonstrated by means of Lyapunov based techniques. Results therein show robustness also in the presence of aerodynamic drag disturbances. Trajectory tracking in the absence of linear velocity measurements has been considered in [15], where a hierarchical controller has

The research of R. Naldi, M. Furci and L. Marconi is framed within the collaborative project SHERPA (Smart collaboration between Humans and ground-aerial Robots for imProving rescuing activities in Alpine environments, ICT 600958) supported by the European Community under the 7th Framework Programme. Research by R. G. Sanfelice has been partially supported by the NSF under CAREER Grant no. ECS-1150306 and by the AFOSR under YIP Grant no. FA9550-12-1-0366.

R. Naldi, M. Furci and L. Marconi are with CASY-DEI, Università di Bologna, Bologna, 40133, Italy, roberto.naldi@unibo.it, michele.furci@unibo.it, lmarconi@unibo.it. R.G. Sanfelice is with the Department of Aerospace and Mechanical Engineering, University of Arizona, Tucson, AZ 85721 - USA, rricardo@u.arizona.edu. Corresponding author: Roberto Naldi, roberto.naldi@unibo.it.

been proposed. In [16], almost-global stability results are achieved by considering geometric methods and then applied to the control of a quadrotor aerial vehicle. Backstepping control design has been proposed in [17] in order to perform aggressive maneuvers by considering the dynamics of a small-scale helicopter. A global stabilizing controller based on synergistic Lyapunov functions has appeared in [18]. In [19], [20], inner-outer loop control strategies have been employed to stabilize the dynamical model of a miniature helicopter. The proposed methodology takes into account for the feedback interconnection between the inner attitude and the outer position control loops. More recently, a survey describing feedback control design for under-actuated VTOL systems has appeared in [21].

This work proposes an inner-outer loop control strategy in order to let the dynamics of a miniature VTOL vehicle to track a desired trajectory globally with respect to the initial position and attitude configuration. This is achieved by considering recent results regarding attitude control for rigid bodies [22] where the topological obstructions, which prevent to obtain global stability considering continuous feedback [23], are avoided by employing hybrid control techniques [24]. As a result, to analyze the stability properties of the the proposed inner-outer controller, the interconnection of a hybrid system, modeling the closed-loop attitude dynamics, and a continuous time system, modeling the closed-loop position dynamics, has to be taken into account. More specifically, a cascade control approach is investigated. The proposed controller is based on the idea of “breaking the loop” between the attitude and the position closed-loop dynamics through a suitable choice of the control torques. As an advantage, the overall stability analysis is simplified since the closed-loop system can be considered as a cascade connection. Simulations obtained considering the dynamical model of a miniature quadrotor prototype show the effectiveness of the proposed results.

The paper is organized as follows. Section II presents the dynamical model for the class of under-actuated aerial vehicles of interest. Section III introduces the control problem which is then addressed in Section IV. Finally, the application of the proposed algorithm to the control of a quadrotor prototype is presented in Section V.

A. Notation and Definitions

Throughout this paper, \mathcal{F}_i and \mathcal{F}_b denote, respectively, an inertial reference frame and a reference frame attached to the center of gravity of the vehicle. With $I_n \in \mathbb{R}^{n \times n}$ we denote the n -dimensional identity matrix. Given sets S_1 and S_2 , the

notation $f : S_1 \rightrightarrows S_2$ denotes a set-valued map mapping subsets of S_1 onto subsets of S_2 . With e_1, e_2 and e_3 we denote the unit vectors $e_1 := [1, 0, 0]^T$, $e_2 := [0, 1, 0]^T$ and $e_3 := [0, 0, 1]^T$. For any $x \in \mathbb{R}^3$, we let

$$S(x) := \begin{bmatrix} 0 & -x_3 & x_2 \\ x_3 & 0 & -x_1 \\ -x_2 & x_1 & 0 \end{bmatrix}$$

be a skew-symmetric matrix and we denote with \wedge the inverse operator such that $S(x)^\wedge = x$. Given a rotation matrix $R \in SO(3)$, $\Theta(R) := \frac{1}{2}\text{trace}(I_3 - R)$. With S_n we denote the n -dimensional unit sphere defined as $S_n := \{x \in \mathbb{R}^{n+1} : \|x\| = 1\}$. A unit quaternion $q \in S_3$ is defined as a pair $q = [\eta, \epsilon^T]^T$ in which $\eta \in \mathbb{R}$ and $\epsilon \in \mathbb{R}^3$ are denoted respectively as the scalar and vector part. Given unit quaternions $q_1 = [\eta_1, \epsilon_1^T]^T$ and $q_2 = [\eta_2, \epsilon_2^T]^T$, the standard quaternion product is defined as

$$q_1 \otimes q_2 = \begin{bmatrix} \eta_1 & -\epsilon_1^T \\ \epsilon_1 & \eta_1 I_3 + S(\epsilon_1) \end{bmatrix} \begin{bmatrix} \eta_2 \\ \epsilon_2 \end{bmatrix}.$$

With $\mathbf{1} = [1, 0, 0, 0]^T \in S_3$ we denote the identity quaternion element and, for a quaternion $q = [\eta, \epsilon^T]^T \in S_3$, with $q^{-1} = [\eta, -\epsilon^T]^T$ the inverse, so that $q \otimes q^{-1} = q^{-1} \otimes q = \mathbf{1}$.

We refer to a *saturation function* as a mapping $\sigma : \mathbb{R}^n \rightarrow \mathbb{R}^n$ such that, for $n = 1$,

- 1) $|\sigma'(s)| := |d\sigma(s)/ds| \leq 2$ for all s ,
- 2) $s\sigma(s) > 0$ for all $s \neq 0$, $\sigma(0) = 0$,
- 3) $\sigma(s) = \text{sgn}(s)$ for $|s| \geq 1$,
- 4) $|s| < |\sigma(s)| < 1$ for $|s| < 1$.

For $n > 1$, the properties listed above are intended to hold componentwise.

II. DYNAMICAL MODEL

The dynamics of a large class of miniature Vertical Take-Off and Landing (VTOL) aerial vehicles, including helicopters, ducted-fan and multi-propeller configurations, can be described by considering the so called *vectored-thrust* (see among others [21], [15]) dynamical model:

$$\begin{aligned} M\ddot{p} &= -u_f R e_3 + M g e_3 \\ \dot{R} &= R S(w) \\ J\dot{w} &= S(Jw)w + u_\tau \end{aligned} \quad (1)$$

in which $p = [x, y, z]^T \in \mathbb{R}^3$ denotes the position of the center of gravity of the system expressed in the inertial reference frame \mathcal{F}_i , $w = [w_x, w_y, w_z]^T \in \mathbb{R}^3$ is the angular speed expressed in the body frame \mathcal{F}_b , $R \in SO(3)$ is the rotation matrix relating vectors in \mathcal{F}_b to vectors in \mathcal{F}_i , $M \in \mathbb{R}_{>}$ and $J \in \mathbb{R}^{3 \times 3}$ (with the property that $J = J^T > 0$) are the mass and the inertia matrix of the system, $u_f \in \mathbb{R}_{\geq 0}$ denotes the control force generated by the aircraft own actuators (which, by construction, is directed along the body z axis) and, finally, $u_\tau \in \mathbb{R}^3$ is the control torque vector. In order to model actuator limitations, the control force and torques are required to satisfy $|u_f| \leq f^U > 0$,

$\|u_\tau\| \leq \tau^U > 0$ with f^U, τ^U modeling respectively the maximum attainable force and torques.

Rotations can be parameterized by means of a unit quaternion $q \in S_3$ through the mapping $\mathcal{R} : S_3 \rightarrow SO(3)$ (known as Rodriguez formula [25]) defined as

$$\mathcal{R}(q) = I + 2\eta S(\epsilon) + 2S(\epsilon)^2.$$

The mapping \mathcal{R} is such that $\mathcal{R}(q) = \mathcal{R}(-q)$, namely the two quaternions q and $-q$ corresponds to the same rotation matrix. By employing the quaternion parametrization, the dynamics equation (1) is rewritten as

$$\begin{aligned} M\ddot{p} &= -u_f \mathcal{R}(q) e_3 + M g e_3 \\ \dot{q} &= \frac{1}{2} q \otimes \begin{bmatrix} 0 \\ w \end{bmatrix} \\ J\dot{w} &= S(Jw)w + u_\tau. \end{aligned} \quad (2)$$

III. CONTROL PROBLEM

The goal of the control law to be designed is to track a given time reference position and orientation

$$p_R(t) \in \mathbb{R}^3, \quad R_R(t) \in SO(3) \quad (3)$$

assuming full knowledge of the state of the system. The desired references (3) must be chosen to satisfy the *functional controllability* constraints of the system which are described below. The first constraint derives from the under-actuated nature of system (1) which does not allow to choose a reference position and orientation independently. More specifically, by defining the *reference control force vector* v_R^c as

$$v_R^c(\ddot{p}_R) := M g e_3 - M \ddot{p}_R, \quad (4)$$

the reference attitude $R_R(t) \in SO(3)$ must then satisfy

$$R_R e_3 = \frac{v_R^c(\ddot{p}_R)}{\|v_R^c(\ddot{p}_R)\|}. \quad (5)$$

From a geometrical viewpoint, the above constraint requires the body z -axis of the vehicle to be aligned with the reference control force vector. Note that, to compute a solution to (5)¹, the reference control force vector should be such that

$$\|v_R^c(\ddot{p}_R(t))\| > v^L, \quad \forall t \geq 0 \quad (6)$$

for some $v^L > 0$. The force and torque control inputs required to track asymptotically the desired position and orientation are then given by

$$u_{f_R} = \|v_R^c(\ddot{p}_R)\|, \quad u_{\tau_R} = J\dot{w}_R - S(Jw_R)w_R, \quad (7)$$

where $w_R := R_R^T \dot{R}_R^\wedge$ is the reference angular velocity. From (5) it turns out that the reference angular speed and acceleration along the body x and y axis are functions of the reference control vector and its derivatives, namely

$$[w_{R_x}, w_{R_y}]^T := W_{xy} R_R^T \frac{d}{dt} \frac{v_R^c}{\|v_R^c\|},$$

¹Note that solutions to (5) are nonunique. In fact the constraint is fixing only two of the three degrees of freedom characterizing the rotation matrix; cf. [18].

$$[\dot{w}_{R_x}, \dot{w}_{R_y}]^T := W_{xy} \left(-S(w_R) R_R^T \frac{d}{dt} \frac{v_R^c}{\|v_R^c\|} + R_R^T \frac{d^2}{dt^2} \frac{v_R^c}{\|v_R^c\|} \right)$$

in which $W_{xy} \in \mathbb{R}^{2 \times 3}$ has the first and second rows given by $[0, -1, 0]$, $[1, 0, 0]$. On the other hand, angular speed and acceleration along the body z -axis, namely w_{R_z} and \dot{w}_{R_z} , can be chosen arbitrarily without affecting the position tracking objective. Further constraints on the reference position $p_R(t)$ and the reference orientation R_R must be chosen to let the control force and torques computed in (7) satisfy actuator limitations, namely

$$|u_{f_R}(t)| \leq f^U, \quad \|u_{\tau_R}(t)\| \leq \tau^U \quad \forall t \geq 0. \quad (8)$$

In summary $p_R(t)$ and $R_R(t)$ are required to be sufficiently smooth functions of time satisfying appropriate bounds on high order derivatives.

IV. INNER-OUTER LOOP CONTROL STRATEGY : CASCADE APPROACH

In this section a control design capable of addressing the control problem defined in Section III is presented. The proposed solution is based on the idea of obtaining a hierarchical control structure in which the attitude dynamics of the vehicle is designed as an *inner loop* to govern the position dynamics of the system. To achieve this goal the solution proposed in following subsection aims at obtaining a cascade connection between the attitude and the position subsystems through a suitable design of the control inputs.

A. Position Control Law

As a first step, let us consider the position dynamics in (1). By considering the following error coordinates $\bar{p} := p - p_R$, $\dot{\bar{p}} := \dot{p} - \dot{p}_R$, the position error dynamics can be written as

$$M\ddot{\bar{p}} = -u_f R e_3 + M g e_3 - M \ddot{p}_R. \quad (9)$$

To stabilize the origin of (9), we define the *control force vector* as

$$v^c(\bar{p}, \dot{\bar{p}}, \ddot{\bar{p}}_R) := v_R^c(\ddot{p}_R) + \kappa(\bar{p}, \dot{\bar{p}}), \quad (10)$$

with $\kappa(\bar{p}, \dot{\bar{p}})$ a static state feedback law such that $\kappa(0, 0) = 0$. From (10) it is possible to compute the control orientation $R_c := R_R R_c'(\bar{p}, \dot{\bar{p}})$, with $R_c'(\bar{p}, \dot{\bar{p}}) \in SO(3)$ such that

$$R_c'(0, 0) = I_3, \quad R_c'(\bar{p}, \dot{\bar{p}}) e_3 = R_R^T \frac{v^c(\bar{p}, \dot{\bar{p}}, \ddot{p}_R)}{\|v^c(\bar{p}, \dot{\bar{p}}, \ddot{p}_R)\|}. \quad (11)$$

Moreover, following Section III, it is also possible to define the control angular speed as $w_c := R_c^T \dot{R}_c^{\wedge}$. Note that, when $\bar{p} = \dot{\bar{p}} = 0$ the control orientation R_c coincides with the reference attitude R_R defined in Section III.

To avoid singularities in (11), a suitable design of the position control law $\kappa(\bar{p}, \dot{\bar{p}})$ is required so as to guarantee that the magnitude of the force control vector (4) is non vanishing regardless the current position and velocity errors.

Inspired by [20], we focus on the following nested saturation feedback law

$$\begin{aligned} \zeta_1 &:= \bar{p}, & \zeta_2 &:= \dot{\bar{p}} + \lambda_1 \sigma \left(\frac{k_1}{\lambda_1} \zeta_1 \right) \\ \kappa(\bar{p}, \dot{\bar{p}}) &:= \lambda_2 \sigma \left(\frac{k_2}{\lambda_2} \zeta_2 \right) \end{aligned} \quad (12)$$

in which λ_1 , λ_2 , k_1 and k_2 are positive parameters to be tuned. Note that, from (6) and (10), the constraint $\|v^c(\cdot)\| > 0$ can be satisfied by choosing λ_2 sufficiently small.

Finally, the control input u_f is designed as

$$u_f = u_{f_c}(\bar{p}, \dot{\bar{p}}, \ddot{p}_R) := \|v^c(\bar{p}, \dot{\bar{p}}, \ddot{p}_R)\|. \quad (13)$$

B. Attitude Control Law

Let us denote with $q_R, q_c \in S_3$, where $\mathcal{R}(q_R) \equiv R_R$ and $\mathcal{R}(q_c) \equiv R_c$ for all $t \geq 0$, the *reference* and *control quaternion*, respectively. In particular q_R and q_c can be obtained by lifting trajectories in $SO(3)$ to trajectories in S_3 by employing the path-lifting mechanism proposed in [26]. With the control quaternion at hand, it is possible to define the following attitude error coordinates

$$\bar{q} = q_c^{-1} \otimes q, \quad \bar{w} := w - \bar{w}_c \quad (14)$$

with $\bar{w}_c := \mathcal{R}(\bar{q})^T w_c$ and then rewrite the attitude dynamics in (2) as

$$\begin{aligned} \dot{\bar{q}} &= \frac{1}{2} \bar{q} \otimes \begin{bmatrix} 0 \\ \bar{w} \end{bmatrix} \\ J\dot{\bar{w}} &= \Sigma(\bar{w}, \bar{w}_c) \bar{w} + S(J\bar{w}_c) \bar{w}_c - J\mathcal{R}(\bar{q})^T \dot{w}_c + u_\tau, \end{aligned} \quad (15)$$

having defined $\Sigma(\bar{w}, \bar{w}_c) := S(J\bar{w}) + S(J\bar{w}_c) - (S(\bar{w}_c)J + JS(\bar{w}_c))$. Inspired by [22], we consider then the following hybrid controller:

$$u_\tau = u_\tau^{FF}(\bar{q}, w_c, \dot{w}_c) + u_\tau^{FB}(\bar{q}, \bar{w}, \bar{h}) \quad (16)$$

with

$$\begin{aligned} u_\tau^{FF}(\bar{q}, w_c, \dot{w}_c) &= J\mathcal{R}(\bar{q})^T \dot{w}_c - S(J\bar{w}_c) \bar{w}_c \\ u_\tau^{FB}(\bar{q}, \bar{w}, \bar{h}) &= -k_p \bar{h} \bar{e} - k_d \bar{w} \end{aligned} \quad (17)$$

in which k_p , k_d are positive gains and where $\bar{h} \in \{-1, 1\}$ is obtained through the following hybrid system

$$\mathcal{H}_c \quad \begin{cases} \dot{\bar{h}} = 0 & \bar{h} \bar{\eta} \geq -\delta \\ \bar{h}^+ \in \overline{\text{sgn}}(\bar{\eta}) & \bar{h} \bar{\eta} \leq -\delta \end{cases} \quad (18)$$

where $\delta \in (0, 1)$ is the hysteresis threshold and $\overline{\text{sgn}} : \mathbb{R} \rightrightarrows \{-1, 1\}$ is the outer-semicontinuous set-valued map

$$\overline{\text{sgn}} = \begin{cases} \text{sgn}(s) & |s| > 0 \\ \{-1, 1\} & s = 0. \end{cases}$$

C. Closed-Loop Position Error Subsystem

The closed-loop position error dynamics in (9) can be written by means of the (ζ_1, ζ_2) coordinates defined in (12) as

$$\begin{aligned}\dot{\zeta}_1 &= -\lambda_1 \sigma \left(\frac{k_1}{\lambda_1} \zeta_1 \right) \\ M \dot{\zeta}_2 &= -\lambda_2 \sigma \left(\frac{k_1}{\lambda_1} \zeta_2 \right) + k_1 \sigma' \left(\frac{k_1}{\lambda_1} \zeta_1 \right) + \Gamma(\bar{p}, \dot{\bar{p}}, \bar{q}, q_c),\end{aligned}\quad (19)$$

in which

$$\Gamma(\bar{p}, \dot{\bar{p}}, \bar{q}, q_c) := u_{f_c}(\bar{p}, \dot{\bar{p}}, \ddot{\bar{p}}_R) (\mathcal{R}(q_c \otimes \bar{q}) - \mathcal{R}(q_c)) e_3 \quad (20)$$

is considered here as an exogenous input modeling the influence of the attitude error on the position of the system. For the above closed-loop system, the following property holds true.

Proposition 1 Consider the closed-loop position error subsystem (19). Let $k_1, k_2, \lambda_1, \lambda_2$ be chosen as

$$\lambda_i = \epsilon^{(i-1)} \lambda_i^*, \quad k_i = \epsilon k_i^*, \quad i \in \{1, 2\} \quad (21)$$

where k_i^*, λ_i^* are chosen such that

$$\frac{\lambda_2^*}{k_2^*} < \frac{\lambda_1^*}{4}, \quad 4k_1^* \lambda_1^* < \frac{\lambda_2^*}{4}, \quad 6 \frac{k_1^*}{k_2^*} < \frac{1}{24} \quad (22)$$

for all $\epsilon > 0$. Then the system (19) is Input-to State Stable (ISS) with nonzero restriction² $\Delta_u(\epsilon)$ on the input Γ and no restriction on the initial conditions.

D. Closed-Loop Attitude Error Subsystem

By considering (15) with the control torque given by (16), the following closed-loop attitude error subsystem is obtained:

$$\mathcal{H}_a \begin{cases} \dot{\bar{x}} = F(\bar{x}) & \bar{h}\bar{\eta} \geq -\delta \\ \bar{x}^+ \in G(\bar{x}) & \bar{h}\bar{\eta} \leq -\delta \end{cases} \quad (23)$$

where $\bar{x} = [\bar{q}^T, \bar{w}^T, \bar{h}]^T$,

$$F(\bar{x}) := \begin{bmatrix} \frac{1}{2} \bar{q} \otimes \begin{bmatrix} 0 \\ \bar{w} \end{bmatrix} \\ J^{-1} (\Sigma(\bar{w}, \bar{w}_c) \bar{w} - k_p \bar{h} \bar{\epsilon} - k_d \bar{w}) \\ 0 \end{bmatrix}$$

and $G(\bar{x}) := [\bar{q}^T, \bar{w}^T, \overline{sgn}(\bar{\eta})^T]^T$. For the hybrid system \mathcal{H}_a , applying [22][Theorem 5.2], the following result holds true.

Proposition 2 Consider the hybrid system \mathcal{H}_a given by (23). Then for all $k_p > 0, k_d > 0, \delta \in (0, 1)$ the following results hold true

- the compact set \mathcal{A} given by $(\bar{q}, \bar{w}, \bar{h}) \in S_3 \times \mathbb{R}^3 \times \{-1, +1\}$ s.t. $\bar{q} = \bar{h}\mathbf{1}, \bar{w} = 0$ is globally asymptotically stable;

²For a definition of Input-to-State-Stability with restrictions the reader is referred to [20][Appendix B]

- for each maximal solution to \mathcal{H}_a , given $\Delta > 0$ there exists $T_\Delta > 0$ such that $\Theta(\mathcal{R}(\bar{q}(t, j))) \leq \Delta$ for all $t + j \geq T_\Delta, (t, j) \in \text{dom} \bar{x}$.

Remark. By applying the result in [22][Theorem 5.2] it is possible to show that the attitude $\mathcal{R}(q(t))$ of the vehicle converges asymptotically to $\mathcal{R}(q_c(t))$ globally with respect to the initial attitude position and angular velocity. Global stability is obtained by considering a hybrid controller able to overcome the topological obstruction affecting globally stabilizing continuous feedback on $SO(3)$. In addition, the presence of the hysteresis (which can be varied by a suitable choice of δ) ensures robustness to nonzero measurement noise. \triangleleft

E. Inner-Outer Loop Analysis

The overall closed-loop system turns out to be given by a cascade interconnection (see Figure 1) in which the attitude error dynamics (23) influences the position error dynamics (19) through the signal Γ defined in (20). For the closed-loop system the following property holds true.

Proposition 3 Let the references $p_R(t), R_R(t)$ be such that (5)- (8) hold. Then, there exists $\epsilon^* > 0$ such that by tuning the position controller as in Proposition 1 with $\epsilon < \epsilon^*$ and the attitude controller as in Proposition 2, then every maximal solution to the hybrid system corresponding to the interconnection is complete and⁴

$$\lim_{t \rightarrow \infty} (\mathcal{R}(q(t))^T \mathcal{R}(q_R(t)), p(t) - p_R(t)) = (I_3, 0)$$

globally with respect to the initial conditions.

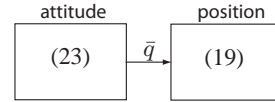


Fig. 1. The interconnection between the closed-loop attitude and position error dynamics.

Remark. Since the control force vector v^c in (10) is given by the sum of the reference control vector v_R^c in (4), which is required to satisfy (6), and the saturated position control law, by choosing ϵ small as in the statement of the proposition it is possible to ensure that the magnitude of v^c is non vanishing. \triangleleft

V. APPLICATION TO THE CONTROL OF A QUADROTOR AERIAL VEHICLE

In order to test the proposed control strategy, the problem of controlling a miniature quadrotor aerial vehicle has been considered.

³For the definition of the domain dom of a solution to a hybrid system, the reader is referred to hybrid systems literature, e.g. [24]

⁴By passing from hybrid time domains to ordinary time.

Following [8], the dynamics of the system can be described by means of (1) in which the resultant force and torques can be computed as a function of the four thrusts T_i , $i = 1, 2, 3, 4$, generated by the four different propellers, namely

$$\begin{bmatrix} u_f \\ u_\tau \end{bmatrix} = \begin{bmatrix} -1 & -1 & -1 & -1 \\ 0 & -d & 0 & d \\ d & 0 & -d & 0 \\ K_{tm} & -K_{tm} & K_{tm} & -K_{tm} \end{bmatrix} \begin{bmatrix} T_1 \\ T_2 \\ T_3 \\ T_4 \end{bmatrix} \quad (24)$$

where b denotes the distance of the propeller spin axis from the center of gravity of the system, and K_{tm} is a parameter which relates the thrust of a single motor to the aerodynamic torque produced along the spin axis of the propeller. The parameters of the specific prototype are $M = 1 \text{ Kg}$, $J = \text{diag}(0.0082, 0.0082, 0.0164) \text{ Kg m}^2$, $d = 0.29 \text{ m}$, $K_{tm} = 0.026$.

In the first simulation, the quadrotor is required to hover at a fixed position starting from an initial attitude configuration in which the system is overturned, namely it has a large initial attitude error. To govern the position dynamics, the controller (12) has been employed by choosing, according to Proposition 1, the control gains as $k_1^* = 1$, $\lambda_1^* = 5$, $k_2^* = 150$ and $\lambda_2^* = 150$. For the attitude loop, the controller in (16)-(18) has been employed with $k_p = 40$, $k_d = 10$. Finally the value of ϵ has been selected equal to 0.2. Figures 2 and 3 show the attitude and the position of the vehicle during the simulation. Note that, despite the large initial attitude error, the final desired configuration is recovered asymptotically. Figure 5 shows the value of the hybrid variable \bar{h} . Observe that, due to the initial conditions close to the jump set, at time $t \approx 0.05$, the value of \bar{h} jumps and a different unit quaternion, representing the same desired hovering orientation, is stabilized. Finally the force and torque control inputs applied to the quadrotor are depicted in Figure 4.

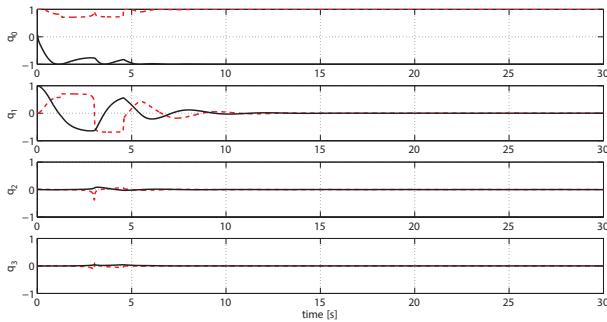


Fig. 2. The attitude trajectory of the quadrotor during the hovering maneuver.

The second simulation considers an aggressive maneuver to be accomplished by the vehicle. In particular the desired time reference signals are given by $x_R(t) := 0$, $y_R(t) := \cos(\gamma t)$, $z_R(t) := -\sin(\gamma t)$, where $\gamma := 2\pi \text{ rad/s}$. The degree of freedom in the choice of R_R is selected in order to maintain the vehicle at a constant heading. The quadrotor

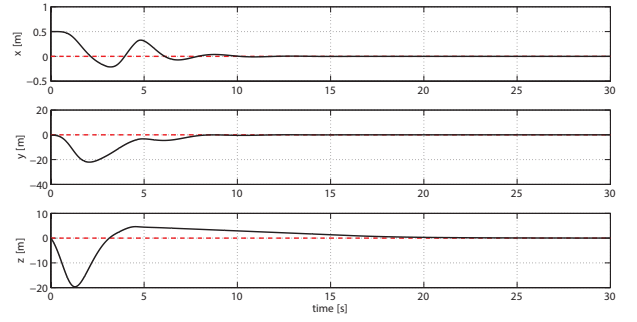


Fig. 3. The position trajectory of the quadrotor during the hovering maneuver.

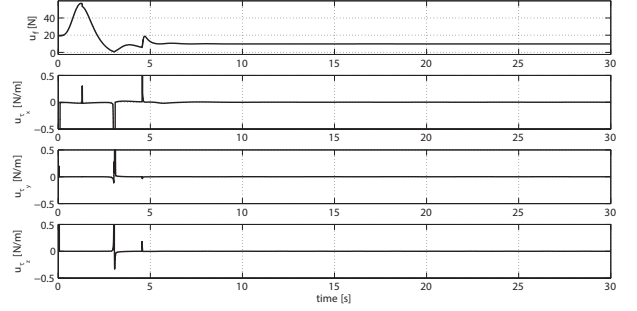


Fig. 4. The control force and torques applied to the quadrotor during the hovering maneuver.

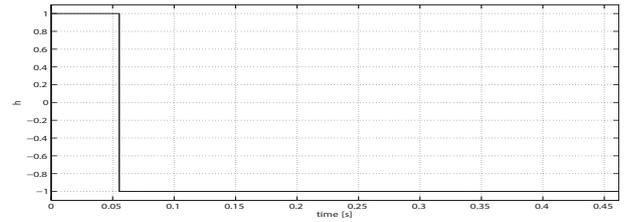


Fig. 5. The hybrid state \bar{h} of the quadrotor during the hovering maneuver.

is required to follow a circular trajectory along the y and z inertial axis at constant speed. For the above references, condition (6) holds with $v^L = \sqrt{(2\pi)^4 + g^2 - 2g(2\pi)^2}$ and hence the constraint requiring that the magnitude of (4) is not vanishing is satisfied since $\sqrt{3}\lambda_2^*\epsilon < v^L$. For this simulation, the attitude controller in (16) is employed with $k_p = 40$, $k_d = 8$. The actual position trajectory and the reference one are depicted in Figure 8, showing how the system converges to the desired path. Figure 6 shows the attitude of the system during the aggressive maneuver. Note that, to compensate for the high centrifugal force, the quadrotor has to continuously rotate (“flip”) around the body x axis. Finally, Figure 7 shows the control force and torques applied to the vehicle during the maneuver.

VI. CONCLUSION

This work has focused on the design of a cascade feedback control strategy able to let the dynamics of an under-actuated VTOL aerial vehicle to track a desired trajectory globally with respect to the initial conditions. This is achieved by considering a hybrid attitude controller, able to overcome

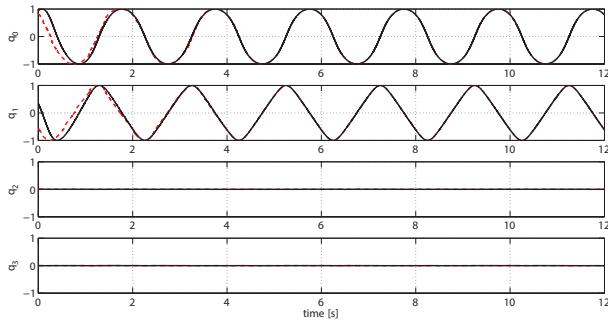


Fig. 6. The attitude trajectory of the quadrotor during the aggressive maneuver.

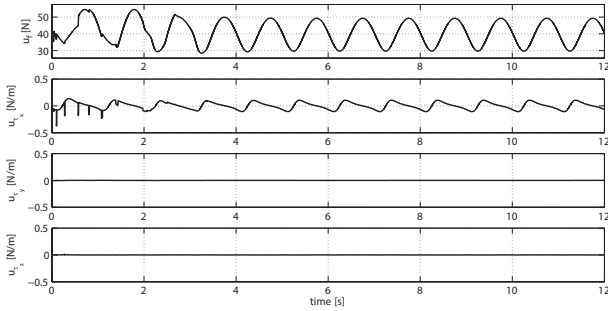


Fig. 7. The control force and torques applied to the quadrotor during the aggressive maneuver.

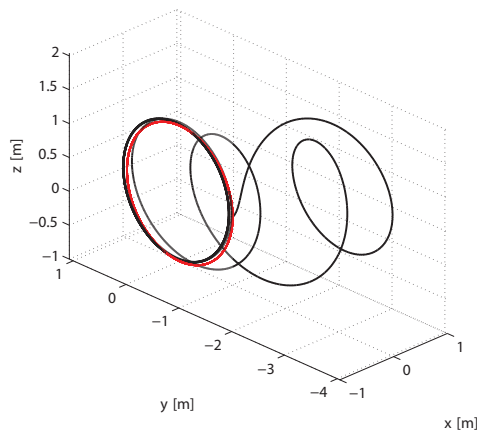


Fig. 8. The position trajectory followed by the quadrotor during the aggressive maneuver.

the well known topological obstructions affecting continuous stabilizing control laws, and by analyzing the interconnection between the attitude and the position closed-loop dynamics. The proposed solution is shown to lead to a cascade connection between a hybrid and a continuous time system. Simulations are finally presented to show the effectiveness of the proposed approach by considering the problem of controlling a miniature quadrotor prototype.

REFERENCES

[1] E. Feron and E.N. Johnson. Aerial robotics. In B. Siciliano and O. Khatib, editors, *Springer Handbook of Robotics*, pages 1009–1027. Springer, 2008.

[2] A. Bachrach, R. He, and N. Roy. Autonomous flight in unknown indoor environments. *International Journal of Micro Air Vehicles*, 1(4):217–228, 2009.

[3] L. Marconi and R. Naldi. Control of aerial robots. hybrid force/position feedback for a ducted-fan. *IEEE Control System Magazine*, 32(4):43–65, 2012.

[4] V. Gavrillets, E. Frazzoli, B. Mettler, M. Piedimonte, and E. Feron. Aggressive maneuvering of small autonomous helicopters: A human-centered approach. *The International Journal of Robotics*, 20(10):795–807, 2001.

[5] J.M. Pfimlin, P. Soueres, and T. Hamel. Hovering flight stabilization in wind gusts for ducted fan UAV. *42nd IEEE Conf. on Decision and Control*, 2004.

[6] R. Naldi, L. Gentili, L. Marconi, and A. Sala. Design and experimental validation of a nonlinear control law for a ducted-fan miniature aerial vehicle. *Control Engineering Practice*, 18(7):747–760, 2010.

[7] R. Naldi and L. Marconi. Robust control of transition maneuvers for a class of V/STOL aircraft. *Automatica*, 49(6):1693 – 1704, 2013.

[8] P. Pounds, R. Mahony, and P. Corke. Modelling and control of a large quadrotor robot. *Control Eng. Pract.*, 18(7):691–699, 2010.

[9] S. Bouabdallah and R. Siegwart. *Advances in Unmanned Aerial Vehicles*, chapter Chapter 6: Design and Control of a Miniature Quadrotor, pages 171–210. Springer Press, Feb. 2007.

[10] R. Cunha, D. Cabecinhas, and C. Silvestre. Nonlinear trajectory tracking control of a quadrotor vehicle. In *Proc. European Control Conference*, 2009.

[11] J. Hauser, S. Sastry, and G. Meyer. Nonlinear control design for slightly non-minimum phase systems: application to V/STOL aircraft. *Automatica*, 28(4):665–679, 1992.

[12] P. Martin, S. Devasia, and B. Paden. A different look at output tracking: control of a VTOL aircraft. *Automatica*, 32(1):101–107, 1996.

[13] T. Koo and S. Sastry. Output tracking control design of a helicopter model based on approximate linearization. In *Decision and Control, 1998. Proceedings of the 37th IEEE Conference on*, volume 4, pages 3635–3640 vol.4, Dec 1998.

[14] M.D. Hua, T. Hamel, P. Morin, and C. Samson. A control approach for thrust-propelled underactuated vehicles and its applications to VTOL drones. *IEEE Transactions on Automatic Control*, 54(8):1837–1853, 2009.

[15] A. Abdessameud and A. Tayebi. Global trajectory tracking control of VTOL-UAVs without linear velocity measurements. *Automatica*, 46(4):1053–1059, April 2010.

[16] T. Lee, M. Leok, and N.H. McClamroch. Nonlinear robust tracking control of a quadrotor UAV on SE(3). *Asian Journal of Control*, 15(3):1–18, May 2013.

[17] E. Frazzoli, M. Dahleh, and E. Feron. Trajectory tracking control design for autonomous helicopters using a backstepping algorithm. *Proceedings of the American Control Conference*, pages 4102–4107, 2000.

[18] P. Casau, R.G. Sanfelice, R. Cunha, D. Cabecinhas, and C. Silvestre. Global trajectory tracking for a class of underactuated vehicles. In *Proceedings of American Control Conference*, pages 419–424, Washington DC, US, 2013.

[19] L. Marconi and R. Naldi. Robust nonlinear full degree of freedom control of an helicopter. *Automatica*, 42:1584–1596, 2007.

[20] A. Isidori, L. Marconi, and A. Serrani. *Robust Autonomous Guidance: An Internal Model Approach*. Advances in Industrial Control. Springer-Verlag London, 2003.

[21] M. Hua, T. Hamel, P. Morin, and C. Samson. Introduction to feedback control of underactuated VTOL vehicles. *IEEE Control Systems Magazine*, 33(2):61–75, February 2013.

[22] C.G. Mayhew, R.G. Sanfelice, and A.R. Teel. Quaternion-based hybrid controller for robust global attitude tracking. *IEEE Transactions on Automatic Control*, 56(11):2555–2566, November 2011.

[23] S.B. Bhat and D.S. Bernstein. A topological obstruction to continuous global stabilization of rotational motion and the unwinding phenomenon. *System & Control Letters*, 39:63–70, 1999.

[24] R. Goebel, R. G. Sanfelice, and A. R. Teel. *Hybrid Dynamical Systems Modeling, Stability, and Robustness*. Princeton University Press, 2012.

[25] M.D. Shuster. A survey of attitude representation. *The Journal of the Astronautical Sciences*, 41(4):439–517, December 1993.

[26] C. Mayhew, R. Sanfelice, and A. Teel. On path-lifting mechanisms and unwinding in quaternion-based attitude control. *IEEE Transactions on Automatic Control*, 58(5):1179–1191.